

The synthetic NCAM mimetic peptide FGL mobilizes neural stem cells in vitro and in vivo

Rebecca Klein · Stefan Blaschke · Bernd Neumaier · Heike Endepols · Rudolf Graf ·
Meike Keuters · Joerg Hucklenbroich · Morten Albrechtsen · Stephen Rees ·
Gereon Rudolf Fink · Michael Schroeter · Maria Adele Rueger

Published online: 10 May 2014
© Springer Science+Business Media New York 2014

Abstract The neural cell adhesion molecule (NCAM) plays a role in neurite outgrowth, synaptogenesis, and neuronal differentiation. The NCAM mimetic peptide FG Loop (FGL) promotes neuronal survival in vitro and enhances spatial learning and memory in rats. We here investigated the effects of FGL on neural stem cells (NSC) in vitro and in vivo. In vitro, cell proliferation of primary NSC was assessed after exposure to various concentrations of NCAM or FGL. The differentiation potential of NCAM- or FGL-treated cells was assessed immunocytochemically. To investigate its influence on endogenous NSC in vivo, FGL was injected subcutaneously into adult rats. The effects on NSC mobilization were studied both via non-invasive positron emission tomography (PET) imaging using the tracer [^{18}F]-fluoro-L-thymidine ([^{18}F]FLT), as well as with immunohistochemistry. Only FGL significantly enhanced NSC proliferation in vitro, with a maximal effect at 10 $\mu\text{g}/\text{ml}$. During differentiation, NCAM promoted neurogenesis, while FGL induced an oligodendroglial phenotype; astrocytic differentiation was neither affected by NCAM or FGL. Those differential effects of NCAM and FGL on differentiation were mediated through different receptors. After FGL-injection in vivo,

proliferative activity of NSC in the subventricular zone (SVZ) was increased (compared to placebo-treated animals). Moreover, non-invasive imaging of cell proliferation using [^{18}F]FLT-PET supported an FGL-induced mobilization of NSC from both the SVZ and the hippocampus. We conclude that FGL robustly induces NSC mobilization in vitro and in vivo, and supports oligodendroglial differentiation. This capacity renders FGL a promising agent to facilitate remyelination, which may eventually make FGL a drug candidate for demyelinating neurological disorders.

Keywords NCAM · NCAM-derived peptide FG Loop · Primary neural stem cells · Remyelination · [^{18}F]FLT · Positron-Emission-Tomography

Introduction

The neural cell adhesion molecule (NCAM) is a membrane-associated glycoprotein that belongs to the immunoglobulin superfamily. NCAM is expressed abundantly throughout the nervous system, where it is involved in development and plasticity, as well as in neuronal survival and differentiation [1, 2]. Amoureux et al. recently reported that NCAM also promotes neurogenesis of hippocampal progenitor cells [3]. Homophilic NCAM binding activates a number of signaling pathways via phosphorylation of the fibroblast growth factor (FGF) receptor [2, 4].

The synthetic NCAM mimetic peptide FG Loop (FGL) encompasses the F- and G-loop region of the second fibronectin type 3 module of NCAM, which interacts with the binding site of FGF receptor 1 [5, 6], thereby mimicking the effect of NCAM on this receptor [2, 7]. FGL was shown to modulate synaptogenesis and presynaptic functions, suggested as the molecular mechanism for cognitive enhancement [8, 9]. In NCAM-deficient mice, depression-like

The two first authors (Rebecca Klein and Stefan Blaschke) contributed equally to this work, thus they share first authorship.

R. Klein · S. Blaschke · M. Keuters · J. Hucklenbroich · G. R. Fink ·
M. Schroeter · M. A. Rueger (✉)
Department of Neurology, University Hospital of Cologne,
Kerpener Strasse 62, 50924 Cologne, Germany
e-mail: adele.rueger@uk-koeln.de

R. Klein · B. Neumaier · H. Endepols · R. Graf
Max Planck Institute for Neurological Research, Cologne, Germany

G. R. Fink · M. Schroeter · M. A. Rueger
Cognitive Neurology Section, Institute of Neuroscience and
Medicine Research Centre Juelich, Juelich, Germany

M. Albrechtsen · S. Rees
Enkam Pharmaceuticals A/S, Copenhagen, Denmark

behavior and reduced hippocampal neurogenesis are reversed by FGL [10]. Skibo et al. suggested a major role for FGL in neuroprotection after stroke in vitro and in vivo [11]. Neuroprotection and induction of neural plasticity may represent treatment approaches for neurological disorders including stroke [12, 13] or neurodegenerative diseases like dementia and Parkinson's diseases [14, 15]. Thus, the aforementioned properties of FGL constitute a promising therapeutic profile for various neurological disorders.

Another therapeutic approach in neurodegeneration and stroke comprises the mobilization of endogenous neural stem cells (NSC) [16]. NSC are physiologically activated in several neurodegenerative disorders like Huntington's or Alzheimer's diseases [17, 18]. Likewise, NSC are mobilized in cerebral ischemia [19]. Unfortunately, those intrinsic processes are insufficient to fully provide self-repair and recovery of function, therefore several attempts have been made to facilitate the intrinsic regenerative capacity of the CNS [20]. Endogenous NSC indeed proliferate in response to various exogenously applied substances such as growth factors or Notch ligands, and contribute to the recovery of function [15, 21–23]. Interestingly, Maric et al. recently suggested that key properties of NSC, namely self-renewal and differentiation, are selectively regulated by signalling through FGF receptors (FGFR) [24]. Moreover, activation of the FGFR is known to keep NSC in an undifferentiated, proliferative state [24, 25].

The effects of FGL on NSC are unknown to date. Given its known mechanisms of action through the FGFR, we hypothesized that FGL should activate and mobilize NSC. We accordingly examined the effects of FGL on endogenous NCS in vitro and in vivo to evaluate the therapeutic potential of this synthetic NCAM-derived peptide.

Material and Methods

Cell culture

NSC culture consisted of fetal rat cortical stem cells derived from embryonic day 14.5 as described previously [26]. The cells were expanded as serum-free monolayer cultures in DMEM/F12 medium (Life Technologies, Darmstadt, Germany) plus N2 supplement (Gibco, Karlsruhe, Germany), penicillin/streptomycin, L-glutamine and sodium pyruvate. FGF2 was included throughout the experiments (10 ng/ml, Invitrogen, Karlsruhe, Germany). After passaging, NSC were re-plated at 10,000 cells per cm [2]. NSC from the first or second passage were used for all experiments.

NCAM (mNCAM-1/CD56, R&D Systems, Minneapolis, USA) at concentrations of 0.1–10 µg/ml, or FGL (Enkam Pharmaceuticals, Copenhagen, Denmark) at concentrations of 5–125 µg/ml, were added to cultures at re-plating. After 16, 24

and 40 h, representative pictures were taken using an inverted fluorescence phase-contrast microscope (Keyence BZ-9000E). Three images were taken per well, cells were counted manually and averaged within the same treatment group.

To assess the proliferation potential of NSC, cells were pre-treated with various concentrations of NCAM (0.1–100 µg/ml) or FGL (0.1–100 µg/ml) for 18 h. Ten µM bromodeoxyuridine (BrdU; Fluka, Munich, Germany) were then added to cultures for 6 h, before NSC were fixed with 4 % paraformaldehyde (PFA) and incubated in 2 N HCl for 30 min for antigen-retrieval. Cells were stained with monoclonal antibody (MAb) against BrdU (clone BU-33, dilution 1:200, Sigma-Aldrich, Munich, Germany) to identify proliferating cells. For visualization, fluorescein-labeled anti-mouse IgG was used (dilution 1:200, Invitrogen, Karlsruhe, Germany); all cells were additionally counterstained with Hoechst 33,342 (Life Technologies, Darmstadt, Germany). To calculate the ratio of proliferating cells, the number of BrdU-positive cells was divided by the total cell number in each sample, and mean values were established among equally treated samples.

The differentiation potential of NCAM- and FGL-treated cells was investigated after withdrawal of the mitogen FGF2 during the expansion phase. After 5 and 10 days of mitogen withdrawal in the presence of 10 µg/ml NCAM or FGL, NSC were fixed, then immunocytochemically stained for markers for neuron specific beta-III tubulin (anti-TuJ1 MAb; dilution 1:100, R&D Systems, Minneapolis, USA), astrocytes (rabbit anti-GFAP; dilution 1:1,000, Abcam, Milton, Great Britain), and oligodendrocytes (mouse anti-CNPase; clone 11-5B, dilution 1:500, Millipore, Billerica, USA). Besides staining for single antigens, double-immunostaining was performed for TuJ1 plus CNPase, in order to identify neurons and oligodendrocytes in the same field of view. For visualization, fluorescein-labeled anti-mouse IgG or anti-rabbit IgG were used (dilution 1:200, Invitrogen, Karlsruhe, Germany); all cells were additionally counterstained with Hoechst 33,342 (Life Technologies, Darmstadt, Germany). To assess the role of the FGFR1 in mediating the differentiation potential of NCAM and FGL, we blocked this receptor with the receptor tyrosine kinase inhibitor PD173074 against FGF and the vascular endothelial growth factor (VEGF) at a concentration of 50 ng/ml (Millipore, Billerica, USA).

All cell culture experiments were performed in triplicate.

Real-time quantitative PCR (RT-qPCR)

RNA from cells was isolated by using the RNeasy Mini Kit (Qiagen, Hilden, Germany). Total RNA concentration and purity were evaluated photometrically. Total RNA was converted to c-DNA by reverse transcription with the Quantitect reverse transcription kit (Qiagen Hilden, Germany). The primer used for Ki67 was obtained from Biolegio (Nijmegen, The Netherlands). The sequence of the primers were: A) forward:

TCTTGGCACTCACAGTCCAG, and B) reverse: GCTGGAAGCAAGTGAAGTCC. The q-PCR reaction was carried out using 10 ng total RNA in a 20 µl reaction Quantitect Reagents (Qiagen, Hilden, Germany) according to the manufacturer's recommendations. The samples were amplified and quantified on a Rotorgene 2000 (Corbett, Sydney, Australia) using the following thermal cycler conditions: activation: 95 °C, 10 min; cycling: 50 cycles, step 1: 92 °C, 15 s, step 2: 52 °C, 15 s, step 3: 72 °C, 40 s. PCR product integrity was evaluated by melting point analysis and agarose gel electrophoresis. Each sample and gene were normalized to RPL13a as reference gene (Yao et al., 2012). Ki67 mRNA levels were normalized to endogenous RPL13a expression (ΔCT); normalized values were then expressed as $2^{-\Delta\text{CT}}$. Mean values were calculated for treated and untreated cells.

Animals and Surgery

All animal procedures were in accordance with the German Laws for Animal Protection and were approved by the local animal care committee as well as local governmental authorities. Spontaneously breathing male adult Wistar rats weighing 270–310 g were anesthetized with 5 % isoflurane. Anesthesia was maintained with 2.5 % isoflurane in a 65/35 % nitrous oxide/oxygen atmosphere. Throughout surgical procedures, body temperature was maintained at 37.0 °C with a thermostatically controlled heating pad.

Subcutaneous injections

In one group ($n=6$) FGL was injected subcutaneously (s.c.) in a concentration of 10 mg/kg body weight for 5 days. As control, $n=6$ rats were sham-injected with 0.9 % saline. After each procedure, all animals were allowed to recover from anesthesia and were put back into their home cages, where they were given access to food and water ad libitum.

BrdU injections

In all animals, the tracer bromodeoxyuridine (BrdU) was injected intraperitoneally (i.p.) to label proliferating cells. Starting on the day of the first FGL- or placebo treatment during same anesthesia, BrdU was injected daily at a concentration of 50 mg/kg body weight for 5 consecutive days, as described previously [26]. This regime resulted in a cumulative dose of 250 mg/kg body weight BrdU per animal.

Positron Emission Tomography (PET)

[^{18}F]-fluoro-L-thymidine ([^{18}F]FLT) was synthesized as described previously [27]. Seven days after initial s.c. injection of FGL or placebo, PET-imaging on $n=3$ FGL- and $n=6$

placebo-treated rats was performed on a microPET Focus 220 scanner (Concorde Microsystems, Inc., Knoxville, TN; 63 image planes; 1.5 mm resolution at the center of the field of view) as described elsewhere [28]. Animals were anesthetized with 5 % isoflurane, maintained with 2 % isoflurane, 65 % nitrous oxide and 35 % oxygen by a respirator system, and placed in the scanner. Temperature was monitored using a rectal probe and maintained at 37 ± 0.5 °C by a thermostatically controlled water flow system (medres, Cologne, Germany). After a 10 min transmission scan for attenuation correction, rats received an intravenous bolus injection of [^{18}F]FLT (1.0–2.3 mCi) into the tail vein. Emission data were acquired for 60 min in list mode. After Fourier rebinning, PET data were reconstructed in 2 time frames of 1800s each using filtered backprojection. Resulting voxel sizes were $0.38\times0.38\times0.82$ mm [3]. The second frame (i.e., minutes 30–60 after tracer injection) was used for image analysis.

Image Analysis

PET images were co-registered to anatomical data of a 3D rat brain atlas [29]. Based on the 3D anatomical data, ellipsoid volumes of interest (VOIs) measuring 4 mm [3] were placed to cover the subventricular zone (SVZ) as well as the dentate gyrus region of the hippocampus in the ipsilateral and contralateral hemisphere. A standard uptake value (SUV) was calculated for each VOI, dividing maximal VOI activity by the decay-corrected injected radioactive dose per body weight. SUV were individually determined and then averaged between animals within each treatment group.

Immunohistochemistry

After PET-imaging, 7 days after FGL or sham treatment, rats were decapitated under deep anesthesia. The brains were rapidly removed, frozen in 2-methylbutane, and stored at -80 °C prior to further histological and immunohistochemical processing. Coronal brain sections (slice thickness 10 µm) were cut at 500 µm intervals and stained with MAb against BrdU to assess proliferating cells (clone BU-33, dilution 1:200, Sigma-Aldrich, Munich, Germany). For antigen-retrieval prior to staining, sections were microwave-heated in 0.01 M citrate buffer, pH 6.0, for 5 min, followed by 2 N HCl at 37 °C for 30 min. For visualization, the ABC Elite kit (Vector Laboratories, Burlingame, USA), with diaminobenzidine (Sigma-Aldrich, Munich, Germany) as the final reaction product, was used. The size of the SVZ was determined for each animal by measuring the area covered by BrdU-positive cells.

To further characterize the proliferating cells in the SVZ, double immunostaining was used. MAb against BrdU labeling proliferating cells was co-stained with anti-SOX2 to label undifferentiated NSC (goat anti-SOX; dilution 1:25; R&D Systems, Minneapolis, USA), and with anti-Iba1 to label

activated non-resting microglia (rabbit anti-Iba1; dilution 1:500; Wako, Richmond, USA). For visualization, fluorescein-labeled anti-goat IgG, anti-mouse IgG and anti-rabbit IgG were used (dilution 1:200, Invitrogen, Karlsruhe, Germany).

Statistical analysis

Descriptive statistics were performed with Microsoft Excel 2003 (Microsoft Corp.). Student's t-tests, one-way ANOVA (followed by Dunnett's post-hoc test) and two-way ANOVA (followed by Holm-Sidak post-hoc test) were performed with SigmaPlot 11.0 for Windows (Systat Software Inc., San Jose, California, USA). Statistical significance was set at $p < 0.05$.

Results

Effects on proliferation and differentiation potential of NSC in vitro

To investigate the effects of NCAM and FGL on NSC in primary monolayer cultures, NSC were treated with NCAM or FGL in various concentrations.

The effect of various concentrations of NCAM or FGL on proliferative activity was first examined using the BrdU incorporation assay. The concentration of NCAM had a significant effect on BrdU incorporation ($F(7,200)=9.85$; $p < 0.001$) with an increased BrdU incorporation into NSC at 5 $\mu\text{g/ml}$ and at 10 $\mu\text{g/ml}$ compared to control (Fig. 1a). FGL led to a

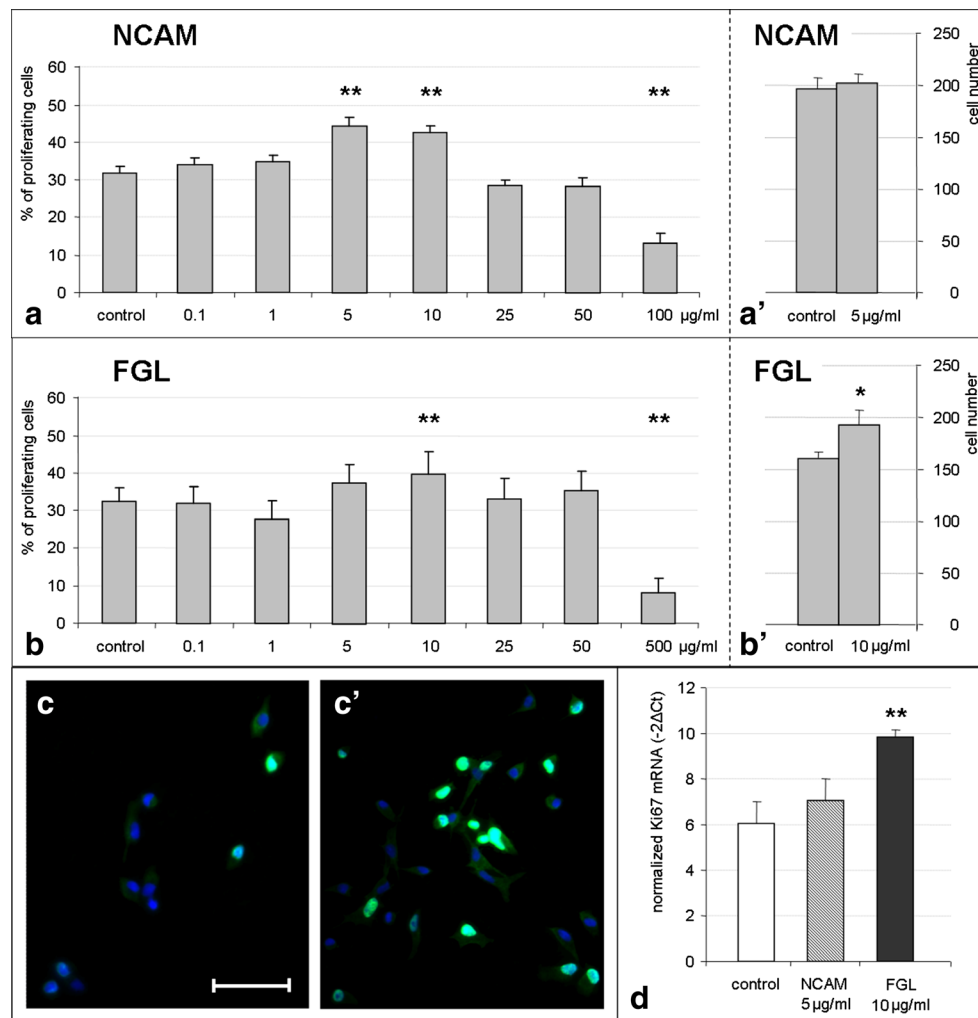


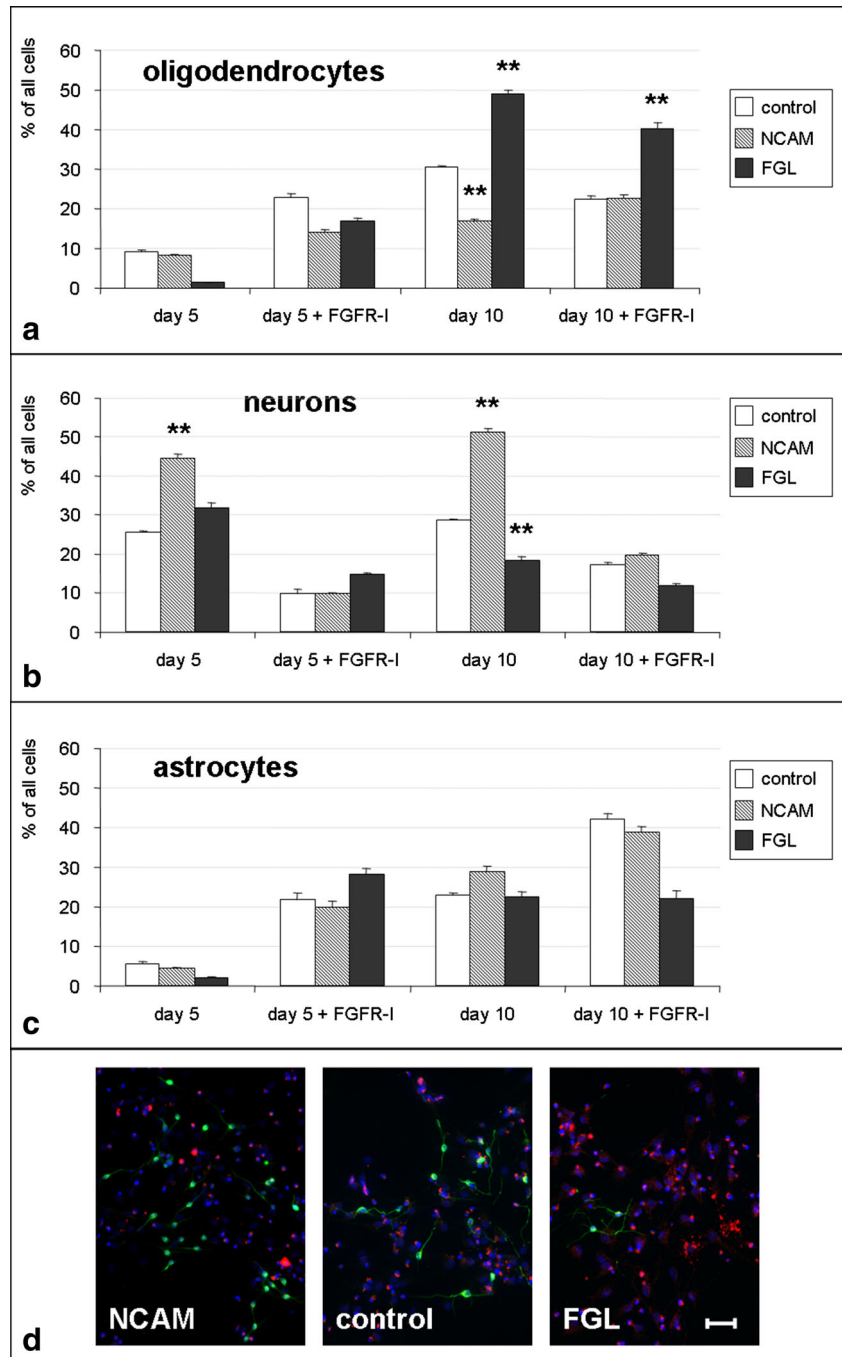
Fig. 1 FGL enhanced NSC proliferation in vitro Fetal rat cortical NSC were exposed to various concentrations of NCAM or FGL. **a** Incorporation of BrdU into NSC was increased after treatment with NCAM at concentrations of 5 and 10 $\mu\text{g/ml}$. In contrast, addition of 100 $\mu\text{g/ml}$ was detrimental to proliferation (** $p < 0.01$). **a'** NCAM treatment for 24 h did not increase absolute NSC numbers. **b** Addition of 10 $\mu\text{g/ml}$ FGL significantly increased the proliferative activity of NSC as measured by BrdU incorporation, while high concentrations (500 $\mu\text{g/ml}$) led to a decrease in proliferation (means \pm SEM; ** $p < 0.01$). **b'** Addition of

10 $\mu\text{g/ml}$ FGL (compared to control) significantly increased the number of NSC within 24 h of treatment (* $p < 0.05$). **c** Representative images are depicted of NSC treated without (**c**) or with 10 $\mu\text{g/ml}$ FGL (**c'**), stained for BrdU-incorporation (green), nuclear staining in blue; scale bar represents 50 μm . **d** Treating NSC with 10 $\mu\text{g/ml}$ FGL, but not 5 $\mu\text{g/ml}$ NCAM, led to a significant increase in Ki67 mRNA; mRNA levels were normalized to endogenous RPL13a expression and calculated by the $2^{-\Delta\text{Ct}}$ method; all data are depicted as means \pm SEM; ** $p < 0.01$

significant increase of BrdU incorporation into NSC at a concentration of 10 $\mu\text{g/ml}$ ($F(7,345)=7.37$; $p<0.001$; Figs. 1b and c'), compared to control (Fig. 1c). High concentrations of 100 $\mu\text{g/ml}$ NCAM and 500 $\mu\text{g/ml}$ FGL led to a significant decrease in proliferation as measured by BrdU incorporation (Figs. 1a and b). The results on NSC proliferation were validated at the mRNA level using real-time quantitative polymerase chain reaction (qPCR) for the proliferation marker Ki67. In line with the data on BrdU incorporation, treatment with 10 $\mu\text{g/ml}$

FGL led to a significant increase in mRNA of Ki67 ($F(3, 12)=22.68$; $P<0.001$; Fig. 1d). However, treatment with 5 $\mu\text{g/ml}$ NCAM did not increase NSC proliferation as measured by Ki67 mRNA (Fig. 1d). In line with the increase in NSC proliferation determined by two independent assays, treatment with FGL at 10 $\mu\text{g/ml}$ for 24 h led to a significant increase in absolute NSC numbers ($p<0.05$; Fig. 1b'). This effect on NSC numbers was not observed after treatment with 5 $\mu\text{g/ml}$ NCAM (Fig. 1a'). This matched the data on Ki67 mRNA.

Fig. 2 During differentiation, NCAM promoted neurogenesis, while FGL directed NSC toward an oligodendroglial fate. The mitogen FGF2 was withdrawn from NSC cultures treated with 10 $\mu\text{g/ml}$ NCAM or FGL to assess their differentiation potential after 5 and 10 days, either in the presence or absence of FGFR-I. **a** By day 10 of differentiation, FGL-treatment compared to control led to an increase in the generation of oligodendrocytes by ~50 %, while NCAM reduced relative oligodendrocyte differentiation from NSC. The effect of FGL on oligodendrocytes was unaffected by FGFR-I (means \pm SEM; $**p<0.01$). **b** After both 5 and 10 days of differentiation, neurogenesis was promoted in NCAM-treated NSC, but relatively reduced by FGL treatment. The effect of NCAM on neurogenesis was annihilated by inhibiting the FGFR (means \pm SEM; $**p<0.01$). **c** Astrocyte generation was not affected by NCAM or FGL. **d** Representative images of NCAM-treated NSC (left), control NSC (middle), and FGL-treated NSC (right), co-stained for their expression of CNPase (red), and TuJ1 (green); scale bar represents 50 μm



To assess the effects of NCAM and FGL on the differentiation potential of NSC, cells were treated with NCAM (10 $\mu\text{g/ml}$) or FGL (10 $\mu\text{g/ml}$) in the presence or absence of FGFR inhibitor (FGFR-I); untreated cells served as control. During the expansion phase, mitogen was withdrawn from cultures to induce differentiation, and cell fate was determined immunocytochemically after 5 and 10 days. To identify cell fate with the same markers at both time-points, we chose the markers suitable for this purpose under our culture conditions. A two-way ANOVA revealed that the factor “time” as well as the factor “treatment” had significant effects on cell fate. Compared to control, generation of neurons increased by ~50 % after NCAM treatment, as assessed immunocytochemically (Figs. 2b and d). In contrast, FGL-treatment led to a relative reduction in neurogenesis ($F(2,111)=18.13$; $p<0.001$ for factor “treatment”; Figs. 2b and d). The effect of NCAM on neurogenesis was blocked in the presence of FGFR-I ($F(2,54)=0.631$; $p=0.54$ for factor “treatment”; Fig. 2b).

Interestingly, 10 days of FGL-treatment significantly increased the generation of CNPase-positive oligodendrocytes from NSC by ~50 %, while NCAM treatment relatively

reduced oligodendrocytic differentiation ($F(2,111)=7.89$; $p<0.001$ for factor “treatment”; Figs. 2a and d). This effect of FGL on the generation of oligodendrocytes was unaffected by blocking FGFR ($F(2,54)=7.748$; $p<0.001$ for factor “treatment”; Fig. 2a).

Moreover, the interaction between the factors “time” and “treatment” indicated that the differentiation kinetics was affected by NCAM and FGL compared to control ($F(4,111)=21$; $p<0.001$). The generation of GFAP-positive astrocytes was not affected by NCAM or FGL ($F(2,111)=2.20$; $p=0.12$ for factor; Fig. 2c) or by blocking with the FGFR-I ($F(2,54)=0.94$; $p=0.397$; Fig. 2c).

Mobilization of endogenous NSC from the niche in vivo

To assess the effects of the synthetic NCAM mimetic peptide FGL on endogenous NSC in vivo, adult male Wistar rats were systemically treated with FGL s.c. for 5 days and compared to sham-treated animals. In parallel, BrdU was repetitively injected to label proliferating cells in vivo. Treatment with FGL led to an enlargement of the subventricular zone (SVZ)

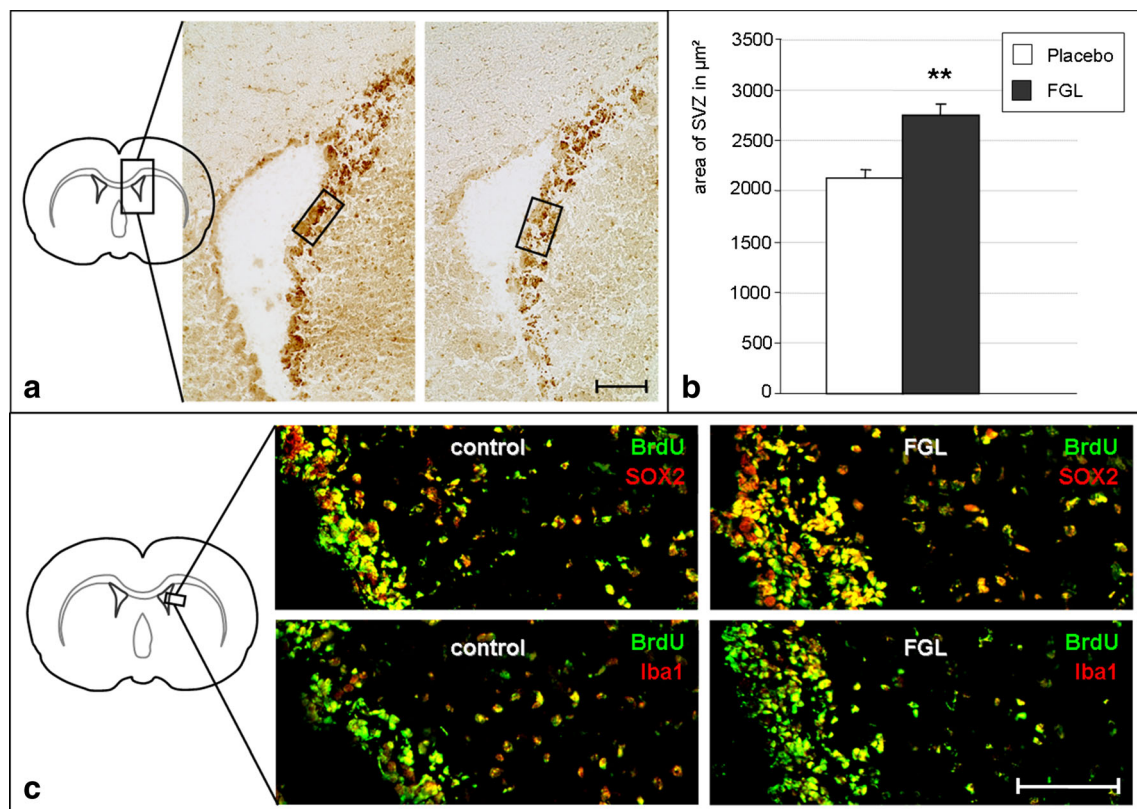


Fig. 3 FGL increased NSC proliferation in the subventricular zone (SVZ) in vivo FGL was injected subcutaneously into naïve rats at 1 mg/kg per day for 5 days. **a** Bromodeoxyuridine (BrdU) given systemically in parallel to FGL-treatment labeled more proliferating cells in the SVZ of FGL-treated rats compared to placebo-injected controls (scale bar represents 50 μm). **b** The size of the SVZ assessed on BrdU-labeled brain sections was significantly increased in FGL-treated animals compared to

placebo-injected controls (means \pm SEM; $**p<0.01$). **c** Representative images of the SVZ and adjacent striatum of control- (left) and FGL-treated rats (right). BrdU-positive proliferating cells in the SVZ co-express SOX2 as a marker of undifferentiated NSC (top). Iba-1 positive microglia are sparsely detected, and localized rather in the striatum than in the SVZ (bottom; scale bar represents 50 μm)

as the major NSC niche, as assessed immunohistochemically *ex vivo* ($p < 0.01$; Figs. 3a and b). We further investigated the nature of those proliferating cells in the SVZ and found them to preferentially express SOX2, a marker for undifferentiated NSC, while co-expression of Iba1, a marker for activated microglia, was limited to a few cells in the striatum (Fig. 3c).

Additionally, mobilization of endogenous NSC from the neurogenic niches was assessed *in vivo* using non-invasive PET-imaging. After one week of FGL treatment, the radiotracer [^{18}F]FLT was systemically injected to label proliferating endogenous NSC *in vivo* before imaging. On PET-images, the brains of FGL-treated rats showed an enhanced accumulation of [^{18}F]FLT in the SVZ ($p < 0.05$; Figs. 4b and c;) compared to placebo-injected control brains (Figs. 4a and c). Additionally, FGL-treated animals displayed significantly more [^{18}F]FLT-accumulation in the hippocampus as compared to control rats ($p < 0.01$; Fig. 4c), indicating a mobilization of proliferating NSC from both NSC niches.

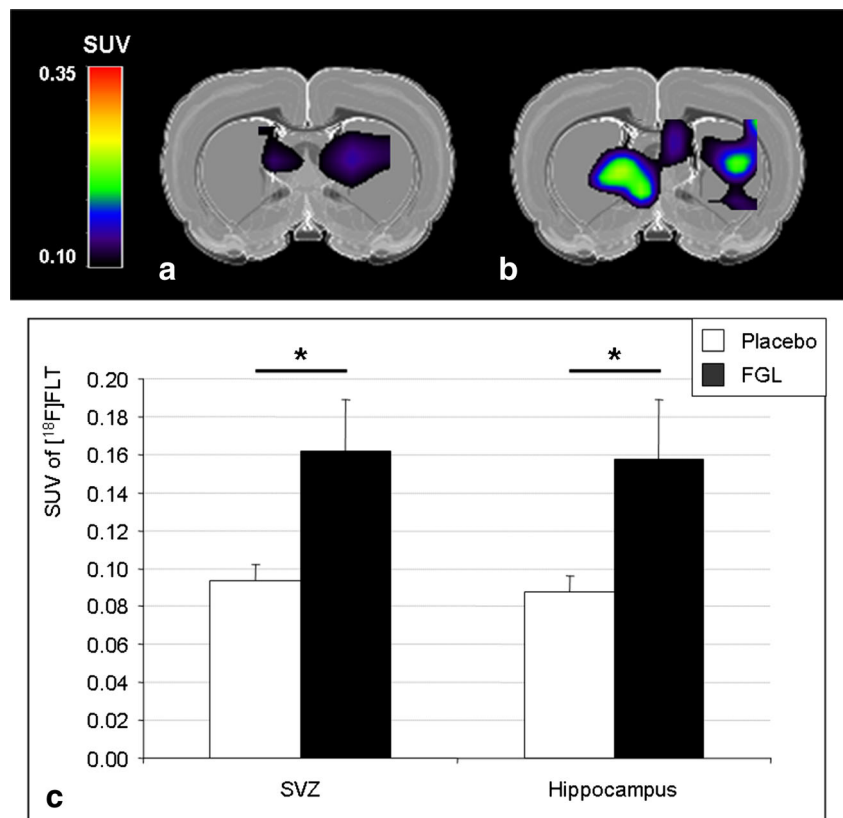
Discussion

For many years, neural stem cell research has attempted to ameliorate neurodegenerative disorders, cerebral ischemia or traumatic injury to brain and spinal cord, via the replacement of lost neurons from (transplanted) neural stem cells. However, stem cell transplantation is associated with many

problems that impede its clinical use, i.e., poor survival of generated neurons, lack of re-integration into neural networks, and potential tumor formation [30–34]. It is now widely acknowledged that beneficial effects described after cell transplantation result rather from the production of restorative factors, neuroprotection, white matter remodeling, the generation of a microenvironment supporting regeneration, and amplification of brain plasticity, than from the generation and re-integration of new neurons [35]. Stem cell activation from the endogenous NSC niche avoids any transplantation-associated complications and therefore represents an alternative therapeutic approach to improve function by facilitating trophic support, regeneration and remyelination [16, 31]. Endogenous NSC are mobilized in various neurodegenerative disorders and stroke [17–19]. Unfortunately, intrinsic processes are *quantitatively* insufficient to enable functionally significant self-repair [20], so that, e.g., pharmacological activation is needed to support the recovery of function [22, 23]. We here found FGL to support oligodendrogenesis rather than neurogenesis, indicating that it might support remyelination. Thus, future studies should address its therapeutic potential in demyelinating disorders.

The NCAM-derived peptide FGL is a small 15-amino-acid-long peptide encompassing the F- and G-loop region of the second fibronectin type 3 module of NCAM that readily enters the CNS after systemic injection [5, 36]. Modulatory effects of FGL on neuronal connectivity, social memory and

Fig. 4 FGL mobilized endogenous NSC in the neurogenic niches of the rat brain *in vivo*. **a** [^{18}F]FLT-PET of a saline-injected control brain compared to **b** rat brain after 5 days of subcutaneous treatment with 1 mg/kg FGL, showing enhanced accumulation of [^{18}F]FLT in the subventricular zone, indicating an increase of proliferating endogenous NSC caused by FGL. **c** FGL-treated rats showed significantly more [^{18}F]FLT-accumulation in the SVZ and the hippocampus than control animals (means \pm SEM; $*p < 0.05$)



behavior via s.c. treatment have been described [10, 36, 37]. The present study provides evidence for a proliferation-inducing effect of FGL on fetal rat cortical stem cells in vitro and in vivo. In contrast, Amoureux et al. recently observed the opposite effect of NCAM on cultured rat hippocampal progenitor cells [3]. A more recent study found no effect of NCAM or FGL on hippocampal progenitor cell proliferation in vivo [10]. We propose that the hippocampal progenitor cells that were subject of those two studies react in a different way from our fetal cortical stem cells, since the former might have already been committed towards a specific (neuronal) fate, while we used non-committed multipotent cells.

With respect to differentiation, NCAM promoted neurogenesis in fetal cortical NSC, which is in line with previous studies showing that NCAM promotes neurogenesis in hippocampal progenitor cells [3, 38]. Somewhat unexpectedly, and contrary to the effect of NCAM, FGL inhibited neurogenesis and promoted the generation of oligodendrocytes. Unlike the effect of NCAM on neurogenesis, this effect of FGL on oligodendrocyte differentiation was not mediated through the FGF receptor 1 (FGFR1). As of yet, FGL has been known to mimic the effects of NCAM via FGFR, both displaying a similar affinity towards FGFR1 and FGFR2, using the FG loop region as common binding site [39]. Nevertheless, our results suggest that NCAM and FGL induce different preferential fate choices in NSC. This observation is in line with a recent report, highlighting that FGL mediates different signaling than FGF, since it activates the downstream signaling molecule FGFR substrate 2 alpha (FRS2alpha) to a lesser extent than the cognate growth factor [5]. The structure of NCAM is quite different from FGL; while NCAM contains five Ig domains and two fibronectin type 3 domains, FGL is part of the second fibronectin type 3 module [40]. It is conceivable that the differential effects of those two molecules on the differentiation potential of NSC are mediated via different binding sites. Further research is warranted to elucidate those binding sites and downstream signaling effects.

Similar to the differential results of NCAM and FGL on NSC differentiation, we found FGL to induce NSC proliferation, while NCAM did not reproducibly show this effect in several independent assays. The proliferation-inducing effect of FGL on NSC in vitro was substantiated in vivo in the present study. Immunohistochemically, those proliferating cells in the SVZ were identified as NSC. Non-invasive imaging using PET and the radiotracer [^{18}F]FLT can be used to visualize and quantify endogenous NSC mobilization by measuring proliferation in the NSC niches in the adult rat brain in vivo [26]. This imaging technique is also capable of quantifying the effects of pharmacological modifications of the stem cell niche [41]. Here, [^{18}F]FLT-PET corroborated that FGL mobilizes endogenous NSC from both stem cell niches, the SVZ and the

hippocampus, in vivo. This readout of therapeutic efficacy should help to facilitate a translational application of FGL in clinical studies.

In summary, we present evidence that the synthetic NCAM mimetic peptide FGL induces proliferation of NSC in vitro as well as in the adult rat brain in vivo, and supports their differentiation into oligodendrocytes. We propose that FGL constitutes a promising future drug candidate to support regeneration in neurological—and especially demyelinating—disorders.

Acknowledgments This research work has been supported by the European Community's Seventh Framework Programme, project number 2,780,006, "NeuroFGL". We thankfully acknowledge further support by Köln Fortune Program/Faculty of Medicine, University of Cologne, Germany, to SB (253/2012).

Disclosures The authors indicate no potential conflicts of interest.

References

1. Ronn, L. C., Hartz, B. P., & Bock, E. (1998). The neural cell adhesion molecule (NCAM) in development and plasticity of the nervous system. *Experimental Gerontology*, 33(7–8), 853–64.
2. Kiselyov, V. V., Skladchikova, G., Hinsby, A. M., et al. (2003). Structural basis for a direct interaction between FGFR1 and NCAM and evidence for a regulatory role of ATP. *Structure*, 11(6), 691–701.
3. Amoureux, M. C., Cunningham, B. A., Edelman, G. M., & Crossin, K. L. (2000). N-CAM binding inhibits the proliferation of hippocampal progenitor cells and promotes their differentiation to a neuronal phenotype. *The Journal of Neuroscience*, 20(10), 3631–40.
4. Neijendam, J. L., Kohler, L. B., Christensen, C., et al. (2004). An NCAM-derived FGF-receptor agonist, the FGL-peptide, induces neurite outgrowth and neuronal survival in primary rat neurons. *Journal of Neurochemistry*, 91(4), 920–35.
5. Chen, Y., Li, S., Berezin, V., & Bock, E. (2010). The fibroblast growth factor receptor (FGFR) agonist FGF1 and the neural cell adhesion molecule-derived peptide FGL activate FGFR substrate 2alpha differently. *Journal of Neuroscience Research*, 88(9), 1882–9.
6. Ojo, B., Gabbott, P. L., Rezaie, P., et al. (2012). An NCAM Mimetic, FGL, Alters Hippocampal Cellular Morphometry in Young Adult (4 Month-Old) Rats. *Neurochem Res*.
7. Berezin, V., & Bock, E. (2004). NCAM mimetic peptides: Pharmacological and therapeutic potential. *Journal of Molecular Neuroscience*, 22(1–2), 33–9.
8. Cambon, K., Hansen, S. M., Venero, C., et al. (2004). A synthetic neural cell adhesion molecule mimetic peptide promotes synaptogenesis, enhances presynaptic function, and facilitates memory consolidation. *The Journal of Neuroscience*, 24(17), 4197–204.
9. Knafo, S., Venero, C., Sanchez-Puelles, C., et al. (2012). Facilitation of AMPA receptor synaptic delivery as a molecular mechanism for cognitive enhancement. *PLoS Biology*, 10(2), e1001262.
10. Aonurm-Helm, A., Jurgenson, M., Zharkovsky, T., et al. (2008). Depression-like behaviour in neural cell adhesion molecule (NCAM)-deficient mice and its reversal by an NCAM-derived peptide, FGL. *European Journal of Neuroscience*, 28(8), 1618–28.

11. Skibo, G. G., Lushnikova, I. V., Voronin, K. Y., et al. (2005). A synthetic NCAM-derived peptide, FGL, protects hippocampal neurons from ischemic insult both *in vitro* and *in vivo*. *European Journal of Neuroscience*, 22(7), 1589–96.
12. Schroeter, M., Zickler, P., Denhardt, D. T., Hartung, H. P., & Jander, S. (2006). Increased thalamic neurodegeneration following ischaemic cortical stroke in osteopontin-deficient mice. *Brain : a journal of neurology*, 129(Pt 6), 1426–37.
13. Overman, J. J., Clarkson, A. N., Wanner, I. B., et al. (2012). A role for ephrin-A5 in axonal sprouting, recovery, and activity-dependent plasticity after stroke. *Proceedings of the National Academy of Sciences of the United States of America*, 109(33), E2230–9.
14. Perrin, R. J., Fagan, A. M., & Holtzman, D. M. (2009). Multimodal techniques for diagnosis and prognosis of Alzheimer's disease. *Nature*, 461(7266), 916–22.
15. Androutsellis-Theotokis, A., Rueger, M. A., Park, D. M., et al. (2009). Targeting neural precursors in the adult brain rescues injured dopamine neurons. *Proceedings of the National Academy of Sciences of the United States of America*, 106(32), 13570–5.
16. Rueger, M. A., Androutsellis-Theotokis, A. (2013). Identifying endogenous neural stem cells in the adult brain *in vitro* and *in vivo*: novel approaches. Current pharmaceutical design, *in press*.
17. Curtis, M. A., Penney, E. B., Pearson, A. G., et al. (2003). Increased cell proliferation and neurogenesis in the adult human Huntington's disease brain. *Proceedings of the National Academy of Sciences of the United States of America*, 100(15), 9023–7.
18. Jin, K., Peel, A. L., Mao, X. O., et al. (2004). Increased hippocampal neurogenesis in Alzheimer's disease. *Proceedings of the National Academy of Sciences of the United States of America*, 101(1), 343–7.
19. Liu, J., Solway, K., Messing, R. O., & Sharp, F. R. (1998). Increased neurogenesis in the dentate gyrus after transient global ischemia in gerbils. *The Journal of Neuroscience*, 18(19), 7768–78.
20. Kittappa, R., Bornstein, S. R., & Androutsellis-Theotokis, A. (2012). The role of eNSCs in neurodegenerative disease. *Molecular Neurobiology*, 46(3), 555–62.
21. Martens, D. J., Seaberg, R. M., & van der Kooy, D. (2002). *In vivo* infusions of exogenous growth factors into the fourth ventricle of the adult mouse brain increase the proliferation of neural progenitors around the fourth ventricle and the central canal of the spinal cord. *European Journal of Neuroscience*, 16(6), 1045–57.
22. Nakatomi, H., Kuriu, T., Okabe, S., et al. (2002). Regeneration of hippocampal pyramidal neurons after ischemic brain injury by recruitment of endogenous neural progenitors. *Cell*, 110(4), 429–41.
23. Androutsellis-Theotokis, A., Leker, R. R., Soldner, F., et al. (2006). Notch signalling regulates stem cell numbers *in vitro* and *in vivo*. *Nature*, 442(7104), 823–6.
24. Maric, D., Fiorio Pla, A., Chang, Y. H., & Barker, J. L. (2007). Self-renewing and differentiating properties of cortical neural stem cells are selectively regulated by basic fibroblast growth factor (FGF) signaling via specific FGF receptors. *The Journal of Neuroscience*, 27(8), 1836–52.
25. Ma, D. K., Ponnusamy, K., Song, M. R., Ming, G. L., & Song, H. (2009). Molecular genetic analysis of FGFR1 signalling reveals distinct roles of MAPK and PLCgamma1 activation for self-renewal of adult neural stem cells. *Molecular Brain*, 2, 16.
26. Rueger, M. A., Backes, H., Walberer, M., et al. (2010). Noninvasive imaging of endogenous neural stem cell mobilization *in vivo* using positron emission tomography. *The Journal of Neuroscience*, 30(18), 6454–60.
27. Jacobs, A. H., Rueger, M. A., Winkeler, A., et al. (2007). Imaging-guided gene therapy of experimental gliomas. *Cancer Research*, 67(4), 1706–15.
28. Schroeter, M., Dennin, M. A., Walberer, M., et al. (2009). Neuroinflammation extends brain tissue at risk to vital peri-infarct tissue: a double tracer [11C]PK11195- and [18 F]FDG-PET study. *Journal of cerebral blood flow and metabolism : official journal of the International Society of Cerebral Blood Flow and Metabolism*, 29(6), 1216–25.
29. Swanson, L. W. 2003 Brain maps: Structure of the Rat Brain. Elsevier.
30. Freed, C. R., Greene, P. E., Breeze, R. E., et al. (2001). Transplantation of embryonic dopamine neurons for severe Parkinson's disease. *The New England Journal of Medicine*, 344(10), 710–9.
31. Lindvall, O., & Hagell, P. (2001). Cell therapy and transplantation in Parkinson's disease Clinical chemistry and laboratory medicine. *CCLM/FESCC*, 39(4), 356–61.
32. Fukuda, H., Takahashi, J., Watanabe, K., et al. (2006). Fluorescence-activated cell sorting-based purification of embryonic stem cell-derived neural precursors averts tumor formation after transplantation. *Stem cells (Dayton, Ohio)*, 24(3), 763–71.
33. Lindvall, O., & Kokaia, Z. (2011). Stem cell research in stroke: how far from the clinic? *Stroke*, 42(8), 2369–75.
34. Amemori, T., Romanyuk, N., Jendelova, P., et al. (2013). Human conditionally immortalized neural stem cells improve locomotor function after spinal cord injury in the rat. *Stem cell research and therapy*, 4(3), 68.
35. Chopp, M., Li, Y., & Zhang, Z. G. (2009). Mechanisms underlying improved recovery of neurological function after stroke in the rodent after treatment with neurorestorative cell-based therapies. *Stroke*, 40(3 Suppl), S143–5.
36. Secher, T., Novitskaia, V., Berezin, V., Bock, E., Glenhøj, B., & Klementiev, B. (2006). A neural cell adhesion molecule-derived fibroblast growth factor receptor agonist, the FGL-peptide, promotes early postnatal sensorimotor development and enhances social memory retention. *Neuroscience*, 141(3), 1289–99.
37. Popov, V. I., Medvedev, N. I., Kraev, I. V., et al. (2008). A cell adhesion molecule mimetic, FGL peptide, induces alterations in synapse and dendritic spine structure in the dentate gyrus of aged rats: a three-dimensional ultrastructural study. *European Journal of Neuroscience*, 27(2), 301–14.
38. Mistry, S. K., Keefer, E. W., Cunningham, B. A., Edelman, G. M., & Crossin, K. L. (2002). Cultured rat hippocampal neural progenitors generate spontaneously active neural networks. *Proceedings of the National Academy of Sciences of the United States of America*, 99(3), 1621–6.
39. Christensen, C., Lauridsen, J. B., Berezin, V., Bock, E., & Kiselyov, V. V. (2006). The neural cell adhesion molecule binds to fibroblast growth factor receptor 2. *FEBS Letters*, 580(14), 3386–90.
40. Kraev, I., Henneberger, C., Rossetti, C., et al. (2011). A peptide mimetic targeting trans-homophilic NCAM binding sites promotes spatial learning and neural plasticity in the hippocampus. *PLoS ONE*, 6(8), e23433.
41. Rueger, M. A., Muesken, S., Walberer, M., et al. (2012). Effects of minocycline on endogenous neural stem cells after experimental stroke. *Neuroscience*, 215, 174–83.